Comparison of finite-difference seismograms and ray-theory travel times in the elastic SEG/EAGE Salt Model, shot 145

Václav Bucha

Department of Geophysics, Faculty of Mathematics and Physics, Charles University, Ke Karlovu 3, 121 16 Praha 2, Czech Republic, E-mail: bucha@seis.karlov.mff.cuni.cz

Summary

Finite-difference seismograms for a selected shot and five receiver configurations computed in the elastic SEG/EAGE Salt Model during the Next-Generation Seismic Modeling and Imaging project are compared with ray-theory travel times calculated using the SW3D software. Two-point rays and travel times of direct, refracted and reflected P-waves and converted S-waves in the smoothed elastic SEG/EAGE Salt Model are computed.

Keywords

Ray tracing, seismic waves, travel times

1 Introduction

House *et al.* (2004) calculated finite-difference seismograms in an elastic SEG/EAGE Salt Model. The data set available via internet (http://www.ees11.lanl.gov/projects/next-gen) contains seismograms of five receiver configurations for shot 145. Three configurations are simulated marine streamer surveys running in three directions: East, South, West. Two configurations are simulated ocean-bottom cables with cables aligned North-South and East-West.

Bucha (2005) presented comparison of finite-difference and ray-theory seismograms in the elastic SEG/EAGE Salt Model only for two receiver configurations: simulated marine streamer survey running in East direction and simulated ocean-bottom cable with cables aligned East-West. Here we compare finite-difference seismograms and ray-theory travel times for all five receiver configurations computed for shot 145. The plots of travel times are more clear than plots of seismograms of individual elementary waves presented by Bucha (2005).

The smoothed SEG/EAGE Salt Model (Bulant, 2001, 2002, 2004) was supplemented by S-waves and densities according to House, Larsen & Bednar (2000). A more detailed description of the smoothed elastic SEG/EAGE Salt Model and the ray tracing computation steps can be found in Bucha (2005).

The GOCAD program was used for visualization of the 3-D smoothed Salt Model interfaces, shot, receiver configurations and computed rays. The figures in the paper are GOCAD screen snapshots of limited resolution. All computations were performed on a PC equipped with an Athlon 64 3400+ (2.2 GHz) processor and with RedHat Linux operating system.

In: Seismic Waves in Complex 3-D Structures, Report 16 (Department of Geophysics, Charles University, Prague, 2006), pp. 29–46

2 Source and receivers

Ray tracing computations were performed for one shot common for five receiver configurations, marine streamers and ocean bottom cables. In the Next Generation Seismic Modeling and Imaging project, Phase 1, a 17 by 17 grid of shot locations was defined, with a shot spacing of 480 m (House *et al.*, 2004). The grid of shots covered almost the entire salt body of the SEG/EAGE model. We have selected shot number 145 located at the center of the grid.

Figures 1 and 2 show the location of the selected shot and five receiver configurations above the salt body. The shot (magenta sphere) is located in the ocean at a depth of 12m. The three sets of eight lines starting at the shot location represent marine streamer surveys running in East direction (**blue** lines), South direction (**yellow** lines) and West direction (**cyan** lines). Each line consists of 141 groups of one-component hydrophones with a group interval of 24m. Hydrophones are located at a depth of 12m.

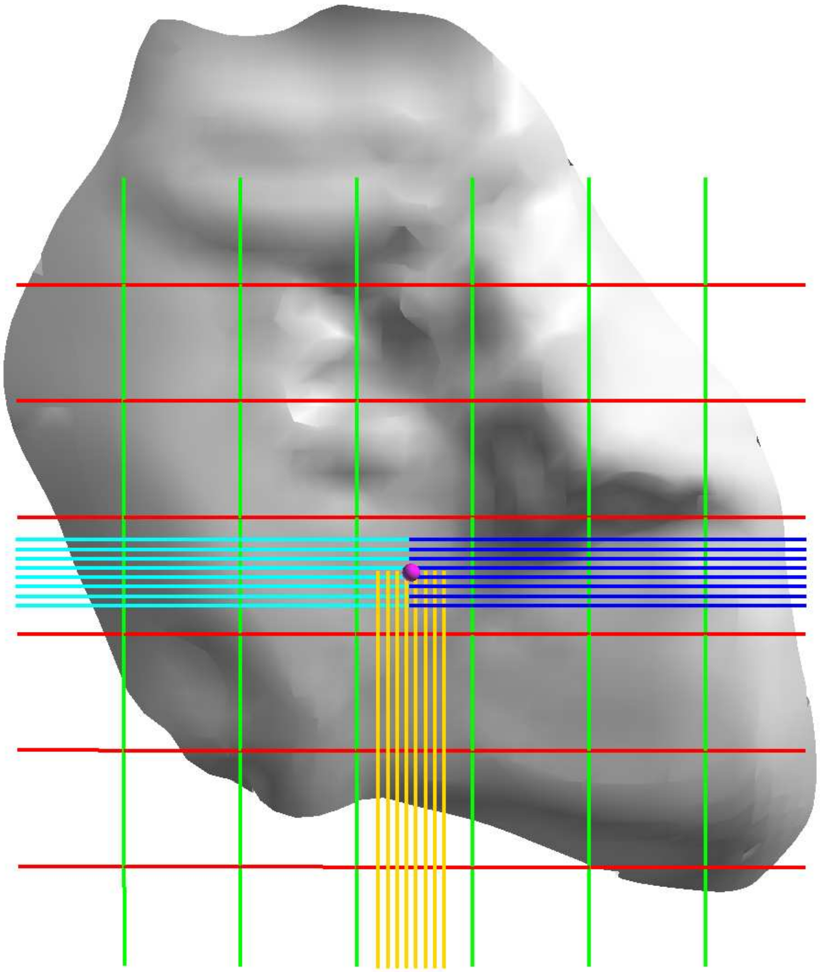

Figure 1. Top view of the shot, five receiver configurations and the salt body.

There are two four component ocean bottom cable configurations, one in North-South direction (six **green** lines) and one in East-West direction (six **red** lines). Each line consists of 281 groups with a group interval of 24m. Each receiver group contains a hydrophone as well as a three-component set of geophones (House, Larsen & Bednar, 2000).

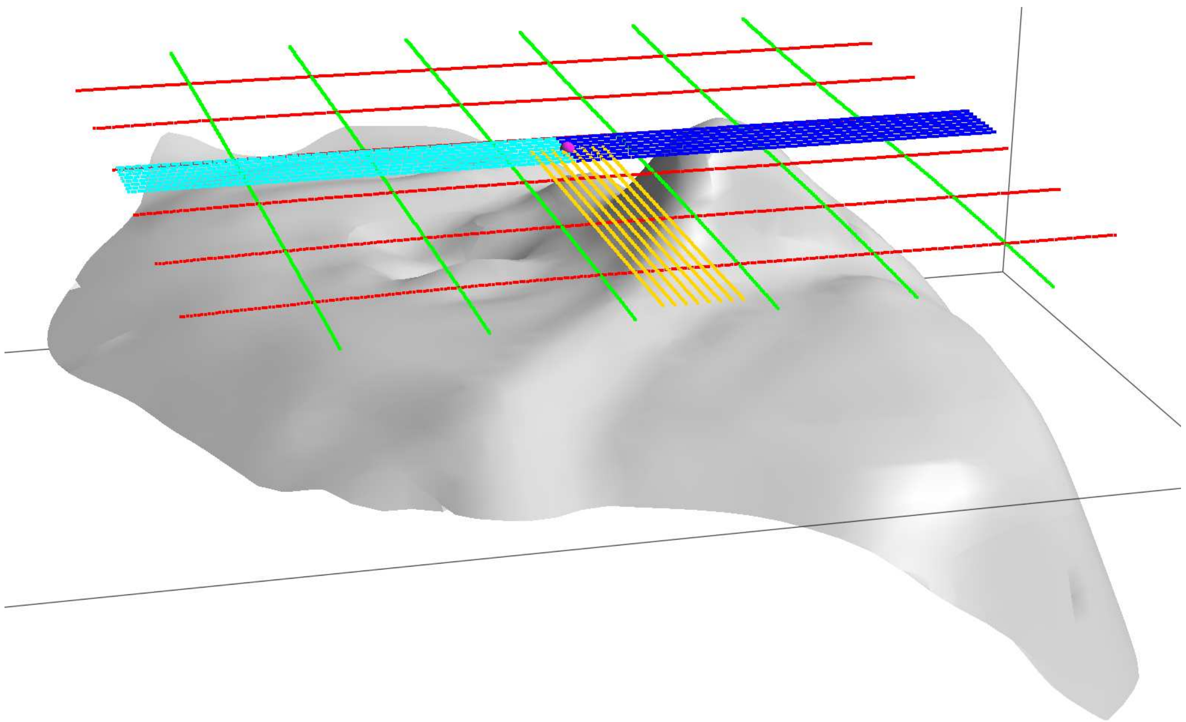

Figure 2. Perspective view of the shot, five receiver configurations and the salt body.

3 Ray tracing computations

Computation of two-point rays and travel times in the elastic smoothed SEG/EAGE Salt Model was performed using the MODEL, CRT and FORMS subroutine packages (Červený, Klimeš & Pšenčík, 1988). The most time-consuming step of the calculation is the two-point ray tracing. Ray tracing output files are then converted to travel times. The two-point rays of the computed waves, shot and receivers are added to the GOCAD files. A more detailed description of the computation steps can be found in Bucha (2005).

3.1 Marine streamer configurations

Two-point rays of 24 elementary waves were calculated for each line of three simulations of marine streamer survey in East, South and West direction.

(1) 18 elementary P-waves: direct wave, wave refracted under the ocean bottom, wave refracted in the salt body, 1x, 2x, 3x, 5x, 10x reflected from the ocean bottom, combinations of wave refracted under the ocean bottom and reflected from the ocean bottom, wave reflected 1x and 2x from the top of salt body, wave reflected from the bottom of the salt body, wave reflected from the bottom interface.

(2) 6 elementary P-waves converted to S-waves and back to P-waves: P-wave reflected and converted to S-wave at the top of the salt body, P-wave refracted and converted to S-wave in the salt body, P-wave reflected and converted to S-wave at the bottom of the salt body, P-wave converted to S-wave at the top of the salt body and reflected from the bottom of the salt body, P-wave converted to S-wave at the bottom ocean interface and reflected from the top of the salt body, P-wave converted to S-wave at the bottom ocean interface and reflected from the bottom of the salt body.

Top interface (sea level) at the depth of 0m is used for storing computed quantities. Receivers are at the depth of 12m and travel times are interpolated from the top interface.

3.2 Ocean bottom cable configuration

Two-point rays of 30 elementary waves were calculated for each line of two simulations of ocean bottom cable survey in North-South and East-West direction.

(1) During the computations of direct P-wave some of the rays were tangent to the weakly curved ocean bottom surface and the computation crashed. The position of receivers is at the ocean bottom. It was necessary to add reference surface near to the ocean bottom, and to project all receiver points onto the reference points "visible" to rays. The travel times were extrapolated from the reference points to the receivers.

(2) 16 elementary waves were stored at the positive ("top") side of the ocean bottom surface. The last reflection before storing was from the sea level.

  (2a) 11 elementary P-waves: 1x, 2x, 4x, 9x reflected from the ocean bottom, combinations of wave refracted under the ocean bottom and reflected from the ocean bottom, wave reflected 1x and 2x from the top of salt body, wave reflected from the bottom of the salt body, wave reflected from the bottom interface.

  (2b) 5 elementary P-waves converted to S-waves and back to P-waves: P-wave reflected and converted to S-wave at the top of the salt body, P-wave reflected and converted to S-wave at the bottom of the salt body, P-wave converted to S-wave at the top of the salt body and reflected from the bottom of the salt body, P-wave converted to S-wave at the bottom ocean interface and reflected from the top of the salt body, P-wave converted to S-wave at the bottom ocean interface and reflected from the bottom of the salt body.

(3) 13 elementary waves were stored at the negative ("bottom") side of the ocean bottom surface.

  (3a) 8 elementary P-waves: wave refracted under the ocean bottom, wave refracted in the salt body, combinations of wave refracted under the ocean bottom and reflected from the ocean bottom, wave reflected 1x and 2x from the top of salt body, wave reflected from the bottom of the salt body, wave reflected from the bottom interface.

  (3b) 5 elementary P-waves converted to S-waves: P-wave reflected and converted to S-wave at the top of the salt body, P-wave reflected and converted to S-wave at the bottom of the salt body, P-wave converted to S-wave at the top of the salt body and reflected from the bottom of the salt body, P-wave converted to S-wave at the bottom ocean interface and reflected from the top of the salt body, P-wave converted to S-wave at the bottom ocean interface and reflected from the bottom of the salt body.

4 Comparison of seismograms and travel times

Finite-difference seismograms are read and plotted using the Seismic Unix programs (Cohen & Stockwell, 2004). Plots of finite-difference seismograms correspond to hydrophones for marine surveys and to vertical component for ocean bottom cable surveys. Shots are simulated by air-gun sources, and use a Ricker wavelet with central frequency of 8Hz (House *et al.*, 2004). This frequency represents a compromise between frequency and the amount of computing time required. Seismograms are computed up to the 5s.

Ray-theory travel times were computed for three marine streamer configurations and two ocean bottom cable configurations. Travel times are computed up to the 8s but plotted only up to the 5s for comparison with finite-difference seismograms. The output of ray-tracing program `crt.for` is converted to travel times using program `crtpts.for`. Travel times of individual elementary waves distinguished by colours are plotted by program `sp.for`.

Figures 3 to 17 correspond to different receiver lines. For each line, we compare the finite-difference seismograms with ray-theory travel times. For nine lines, we also display the two point rays of a selected elementary wave. Ray-theory travel times are denoted by CalComp centred symbol + and distinguished by colours. The travel time for the selected elementary wave is plotted with different centred symbol | . The black + denotes direct wave, wave refracted under the ocean bottom, wave refracted in the salt body, red + denotes multiple reflections from the ocean bottom, green + denotes combinations of wave refracted under the ocean bottom and reflected from the ocean bottom, blue + denotes multiple reflections from the top of the salt body, yellow + denotes wave reflected from the bottom of the salt body, cyan + denotes wave reflected from the bottom interface, magenta + denotes P-waves converted to S-waves and back to P-waves.

Figures 3, 4 and 5 show finite-difference seismograms, ray-theory travel times generated from 24 elementary waves and two-point rays of selected elementary wave for marine streamer surveys. Only one line for each direction (East, South and West) is plotted because the distance between lines is 80m and the seismograms are similar.

The distance between ocean bottom cable lines is 996m and the differences between seismograms for each line seem to be interesting. That is why seismograms and travel times of all ocean bottom cable lines in each direction (North-South and East-West) are presented in the paper. Ray-theory travel times are generated from 30 computed elementary waves. Figures 6 to 17 show finite-difference seismograms, ray-theory travel times and for selected lines also two-point rays of selected elementary wave.

Comparison of finite-difference and ray-theory travel times in this paper shows differences. Some of the arrivals of elementary waves are clearly visible, some arrivals are not so clear or are shifted in time or position. The differences can be explained by the following facts:

- ray-theory travel times were computed in the smoothed elastic SEG/EAGE Salt Model,
- application of the source time function, Ricker signal (FD arrival times differ from the travel times),
- ray-theory travel times are computed for limited number of elementary waves.

Detailed comparison of finite-difference seismograms and travel times requires interactive displaying of rays of elementary waves. The ray paths are for some waves very complicated.

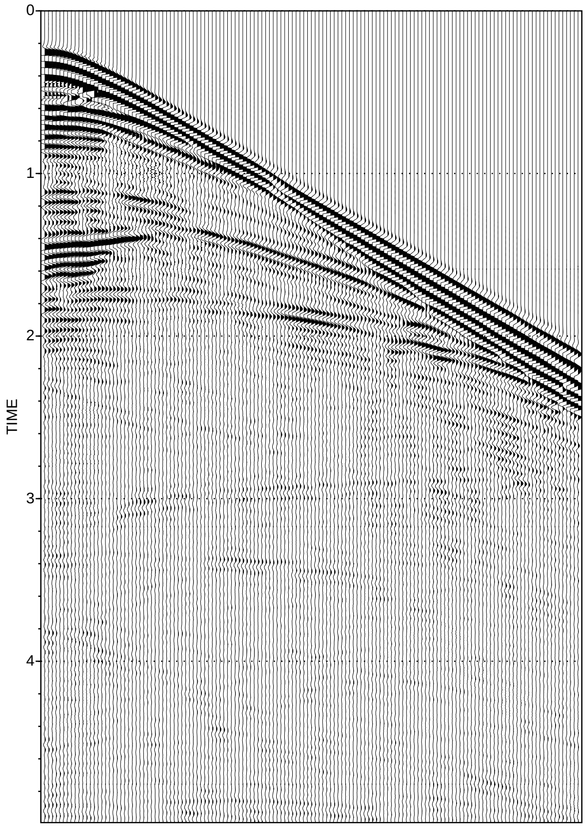

Finite-difference seismograms

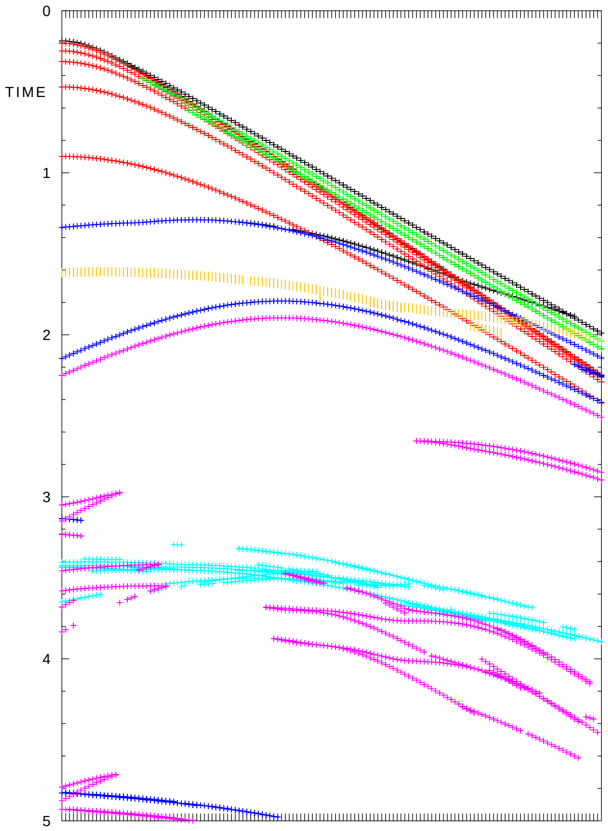

Ray-theory travel times

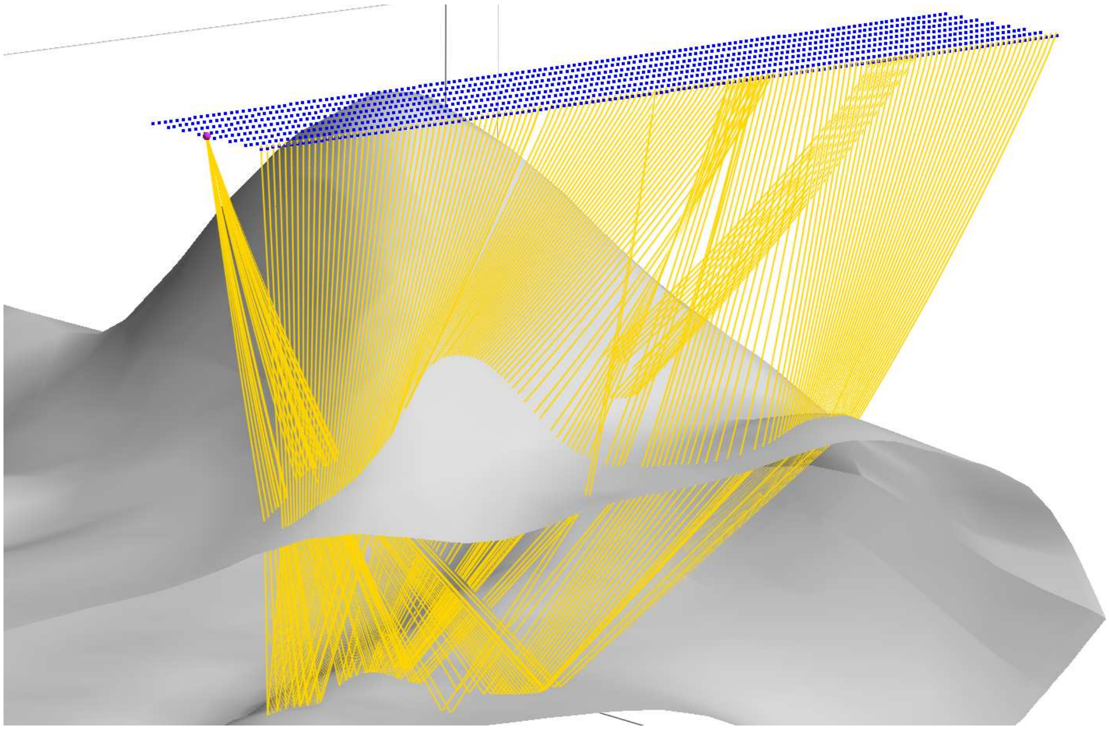

Rays of P-wave reflected from the bottom salt interface.

Figure 3. Marine streamer, East direction, line 1.

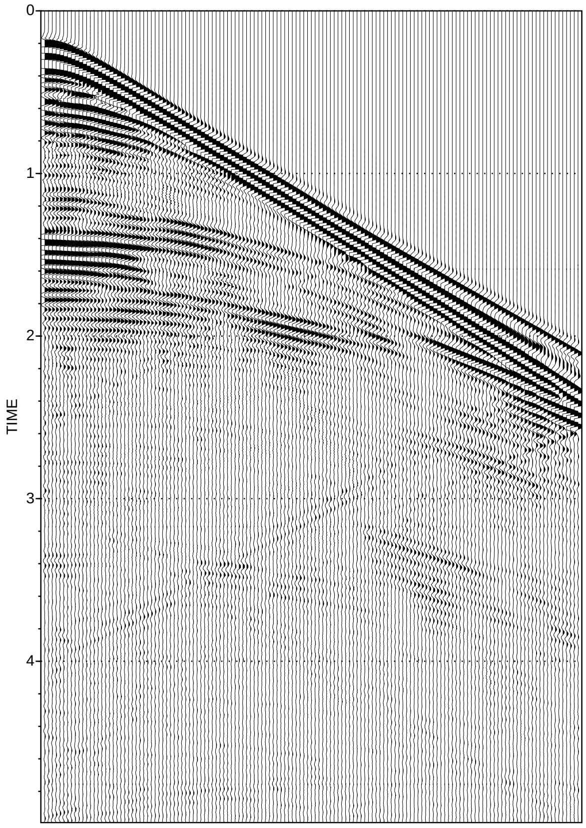

Finite-difference seismograms

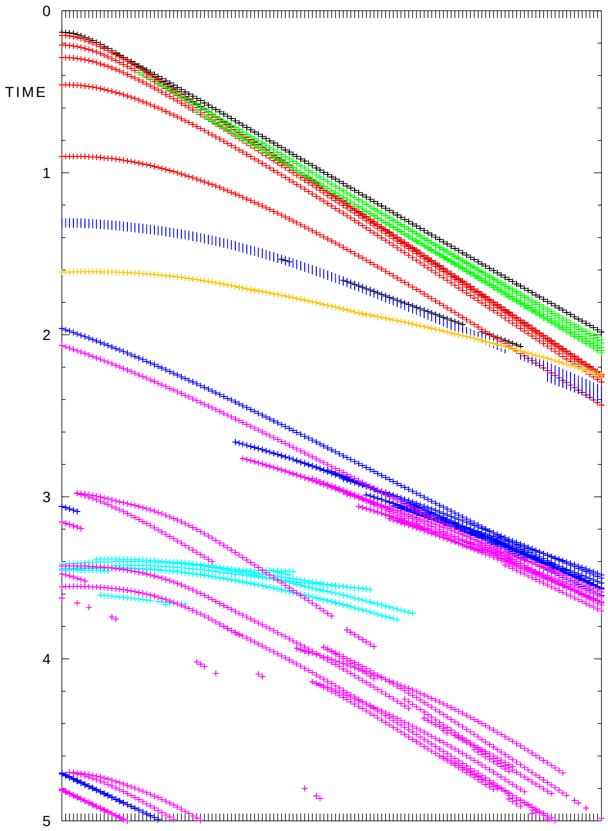

Ray-theory travel times

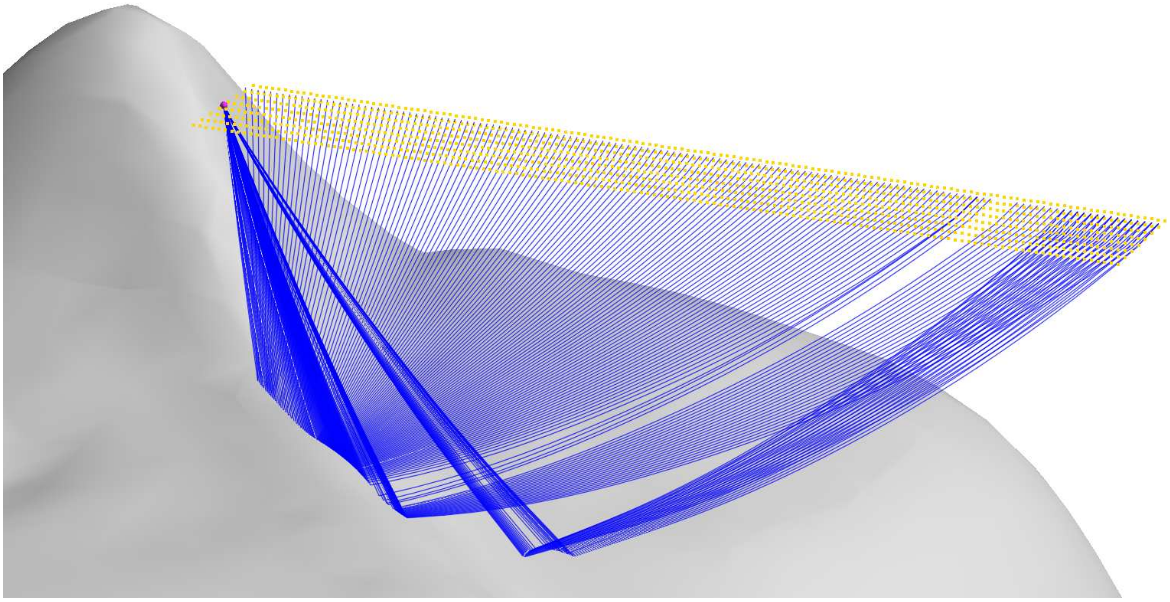

Rays of P-wave reflected from the top salt interface.

Figure 4. Marine streamer, South direction, line 7.

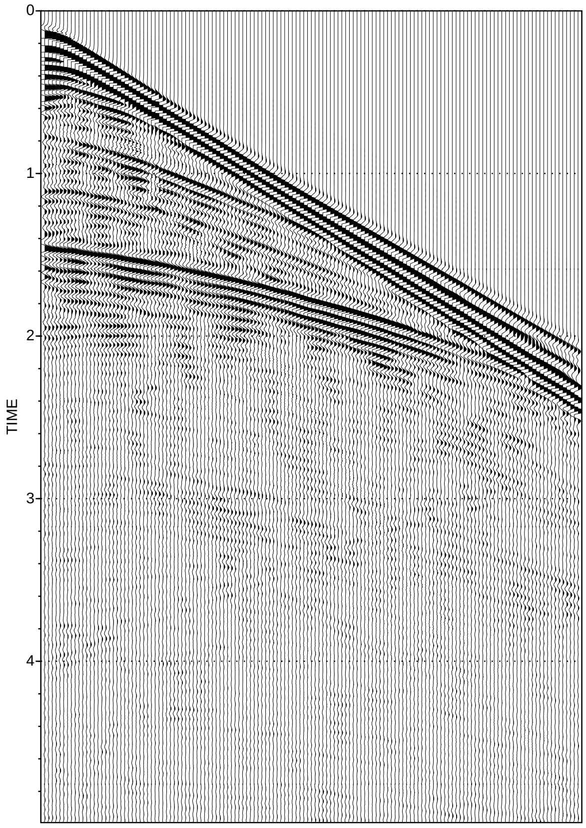

Finite-difference seismograms

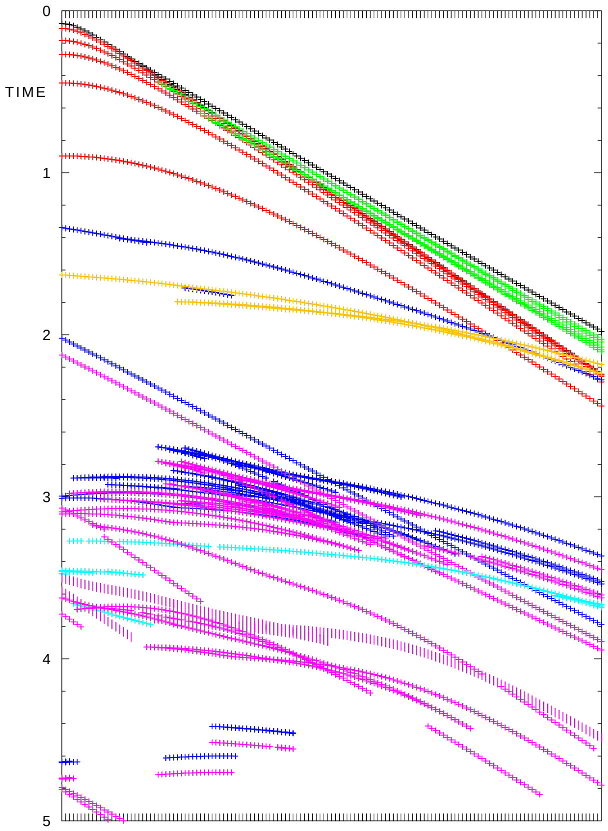

Ray-theory travel times

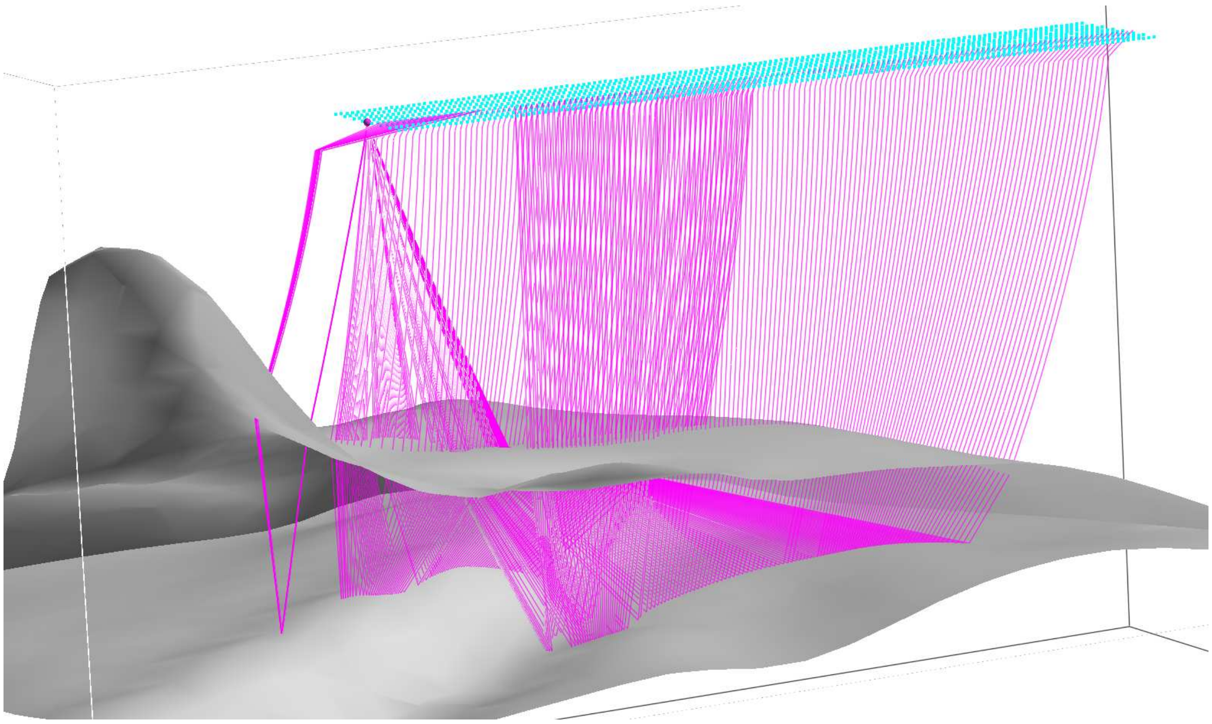

Rays of P-wave reflected and converted to S-wave at the bottom of the salt body.

Figure 5. **Marine streamer, West direction, line 3.**

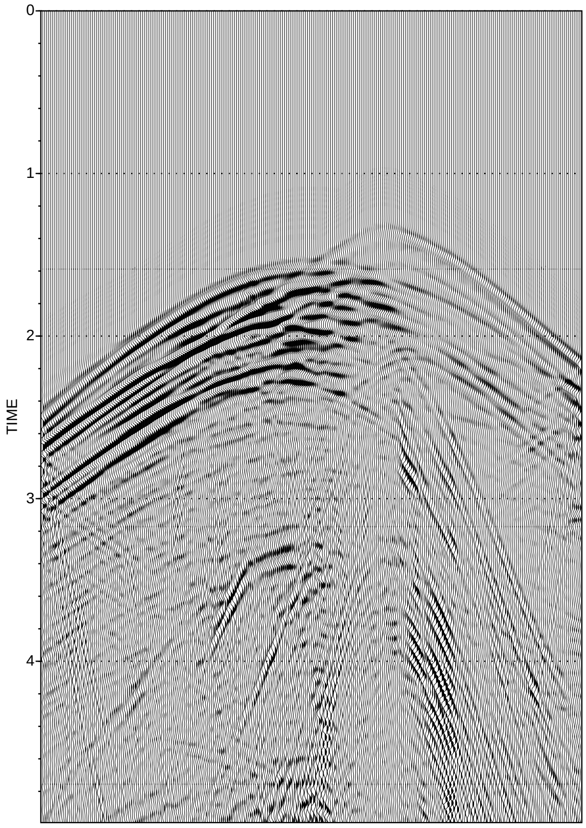

Finite-difference seismograms

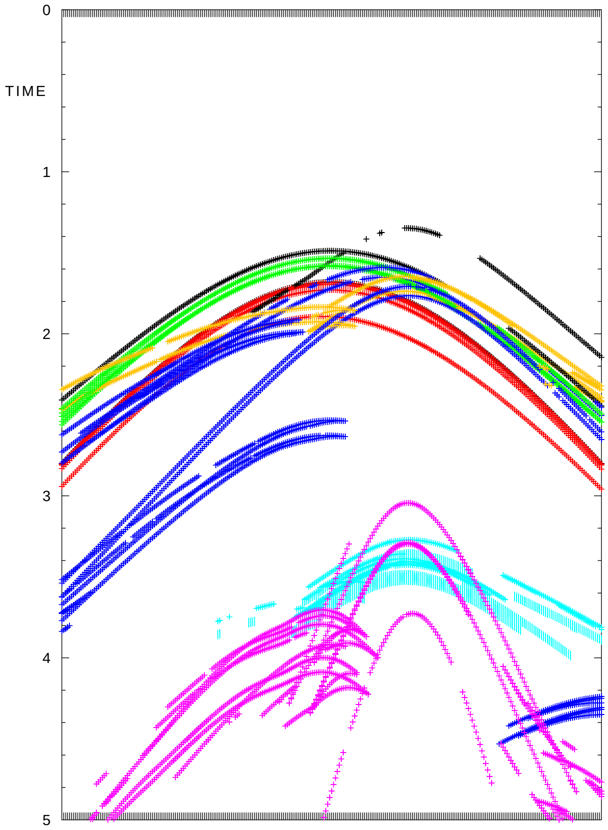

Ray-theory travel times

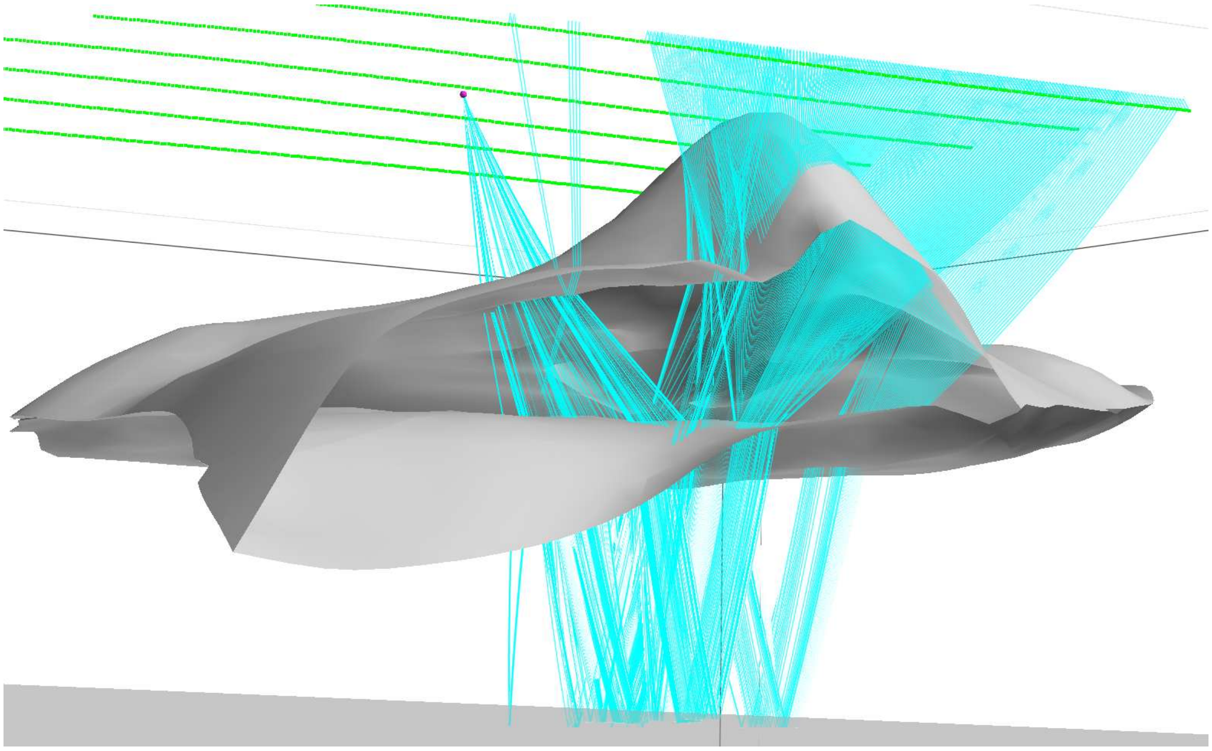

Rays of P-wave reflected from the bottom flat interface and the sea level.

Figure 6. Ocean bottom cable, North-South direction, line 1.

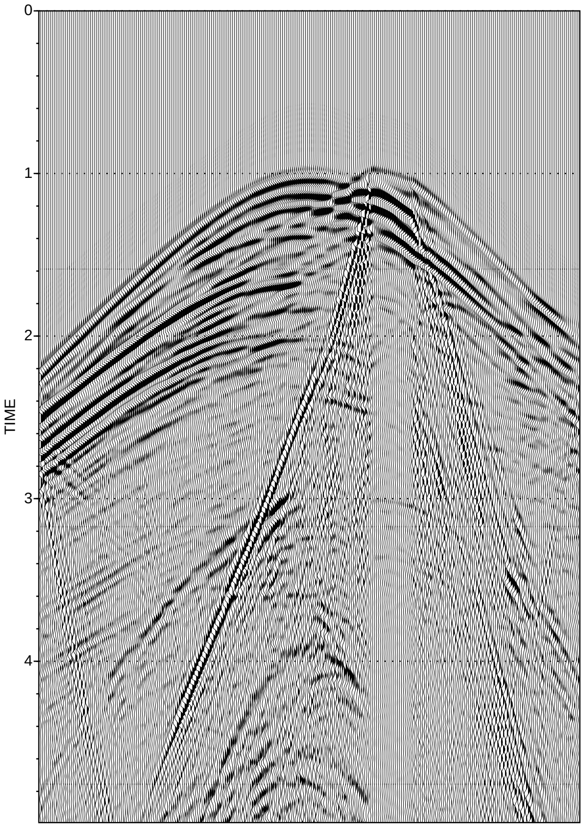

Finite-difference seismograms

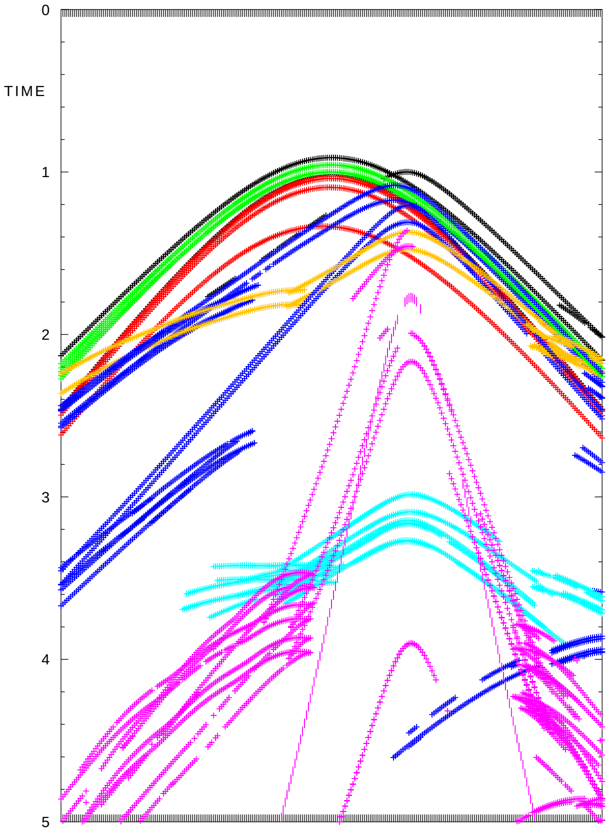

Ray-theory travel times

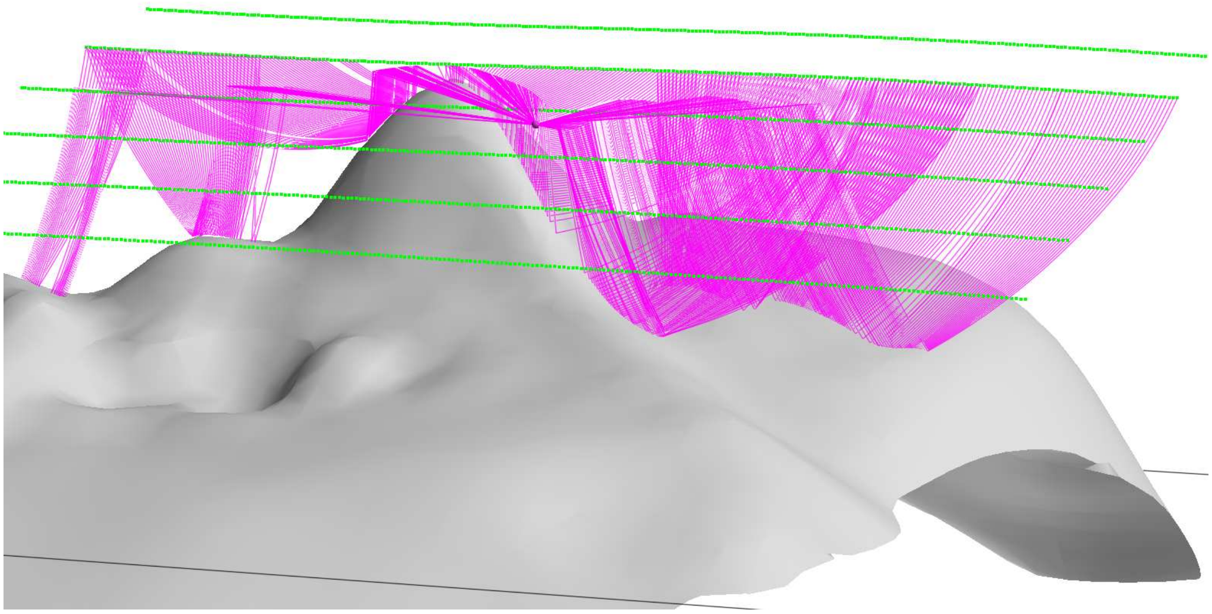

Rays of P-wave converted to S-wave at the bottom ocean interface and reflected from the top of the salt body.

Figure 7. Ocean bottom cable, North-South direction, line 2.

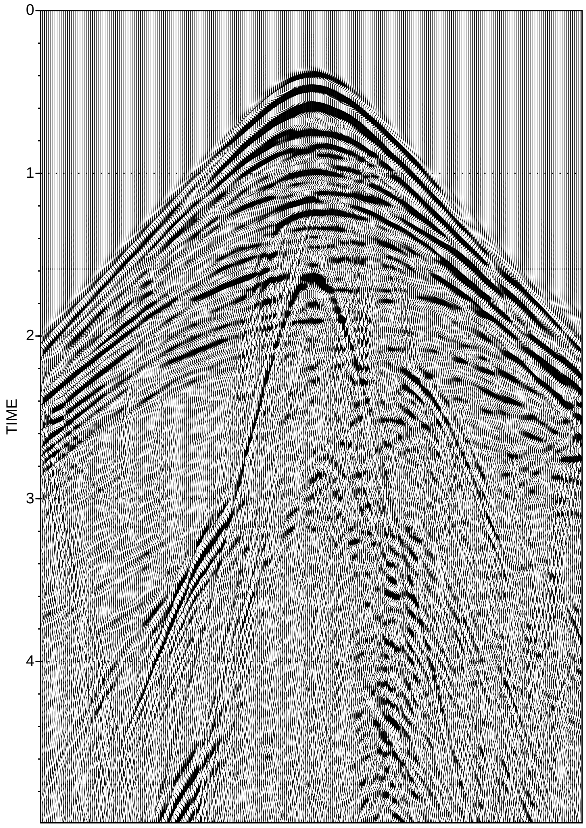

Finite-difference seismograms

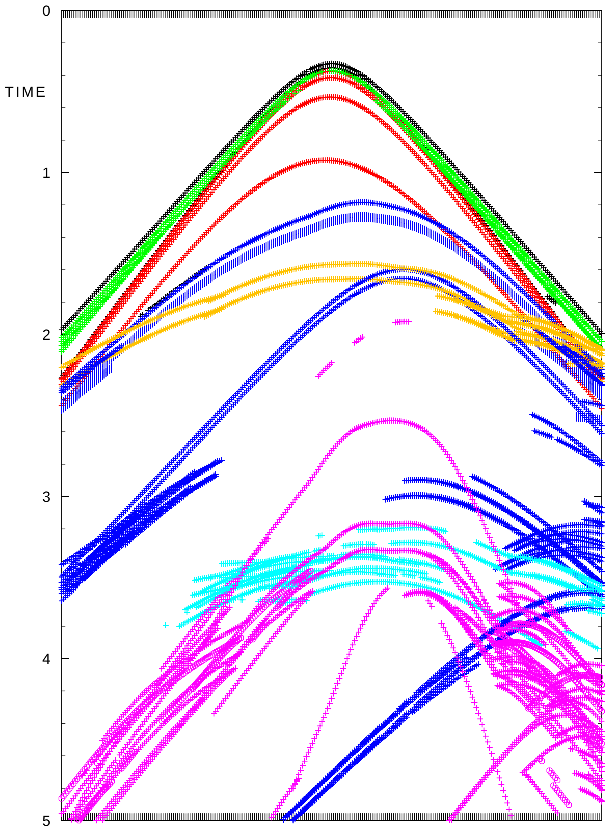

Ray-theory travel times

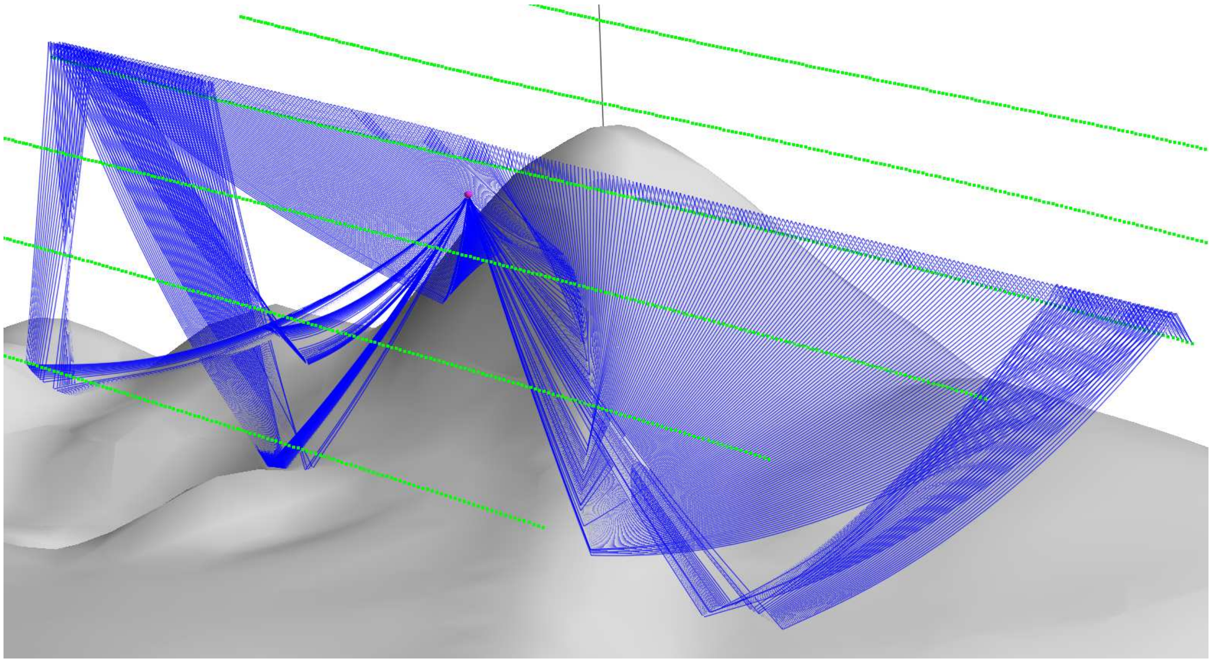

Rays of P-wave reflected from the top of the salt body and sea level.

Figure 8. Ocean bottom cable, North-South direction, line 3.

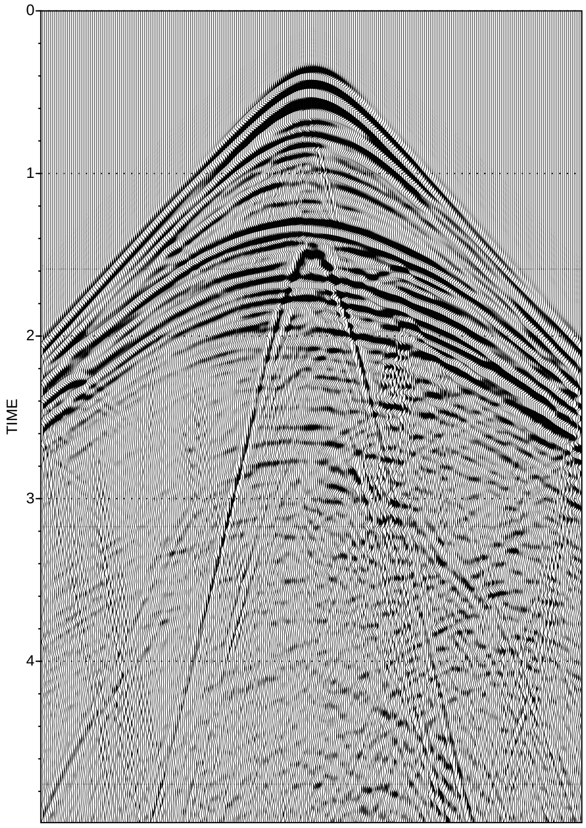

Finite-difference seismograms

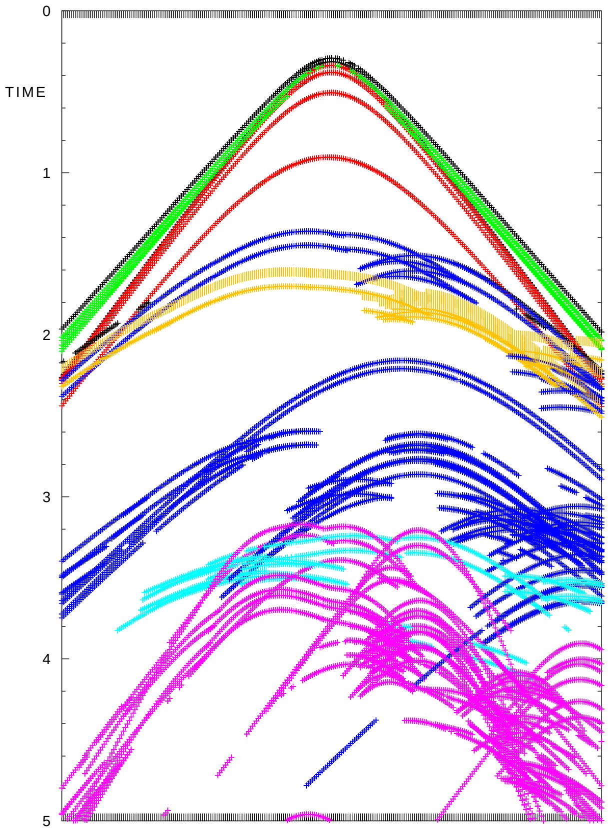

Ray-theory travel times

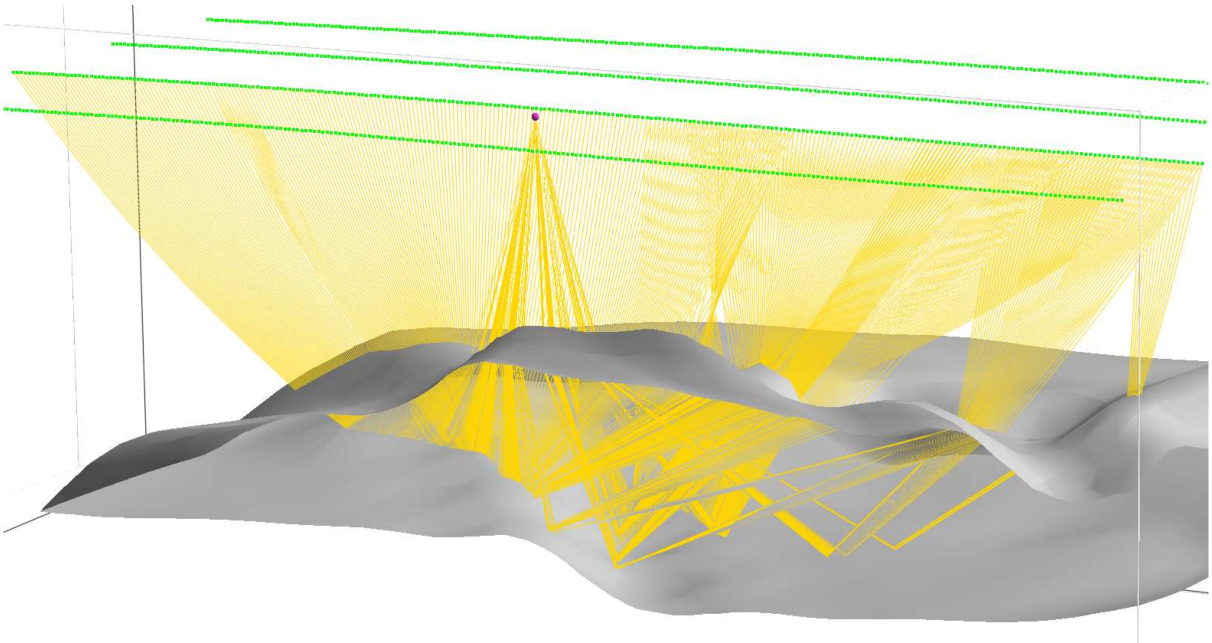

Rays of P-wave reflected from the bottom of the salt body.

Figure 9. Ocean bottom cable, North-South direction, line 4.

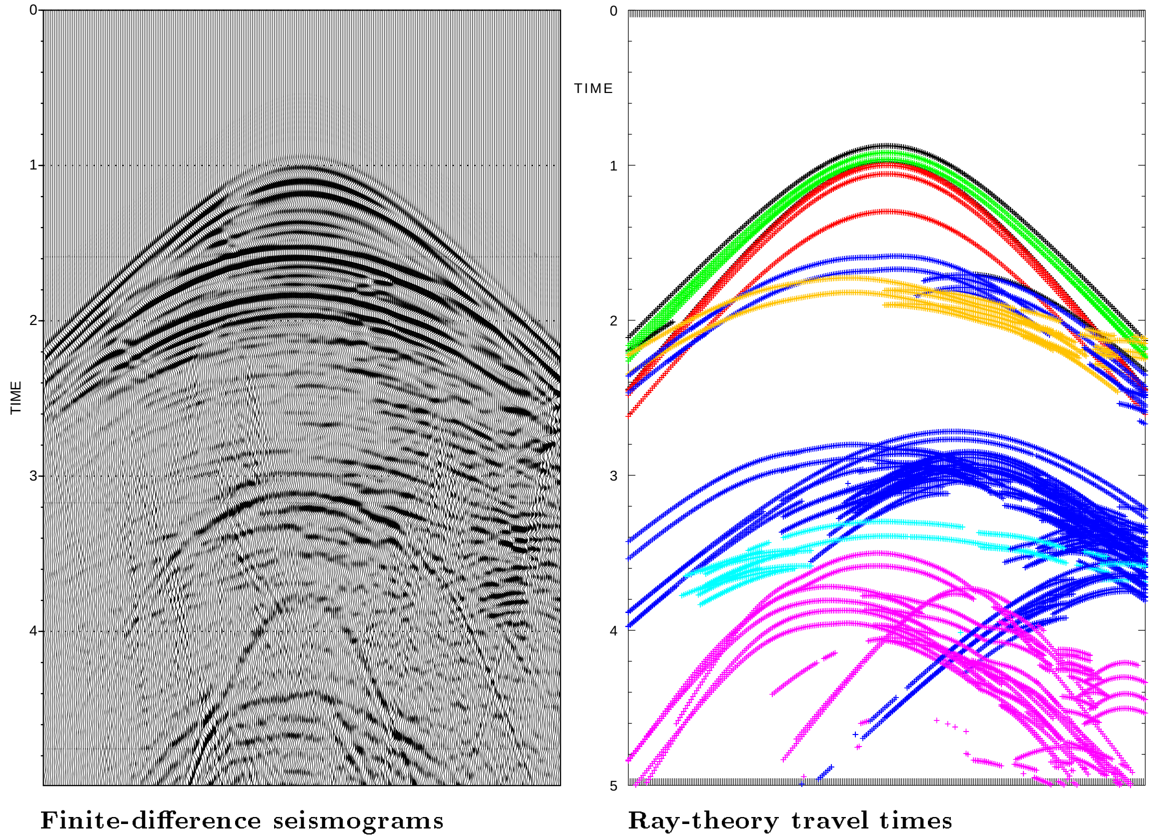

Figure 10. Ocean bottom cable, North-South direction, line 5.

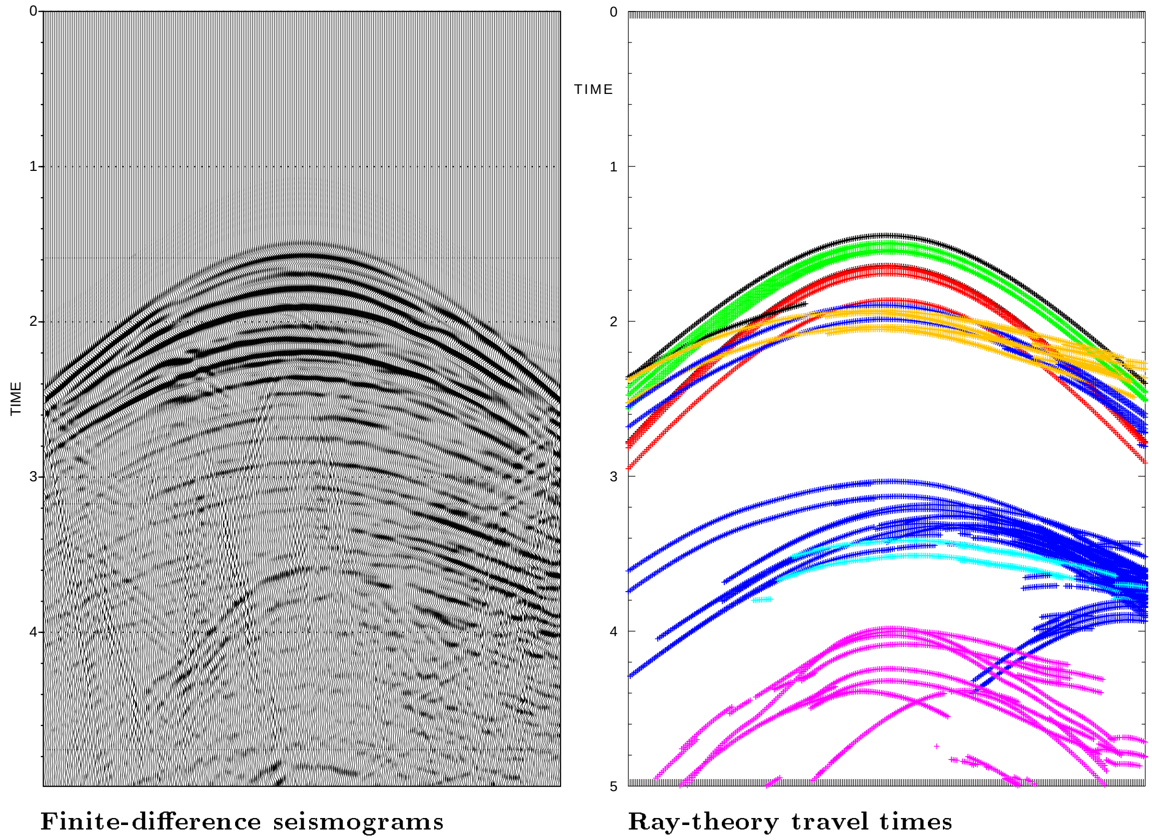

Figure 11. Ocean bottom cable, North-South direction, line 6.

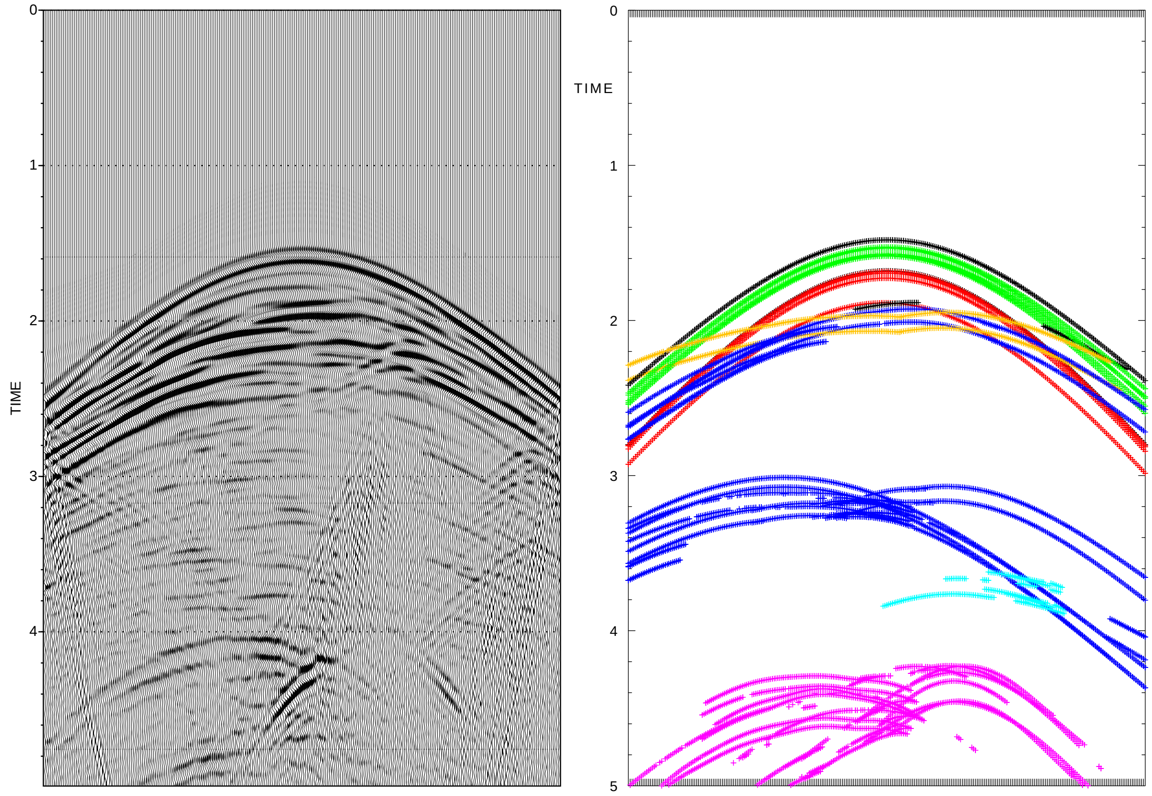

Finite-difference seismograms **Ray-theory travel times**

Figure 12. Ocean bottom cable, East-West direction, line 1.

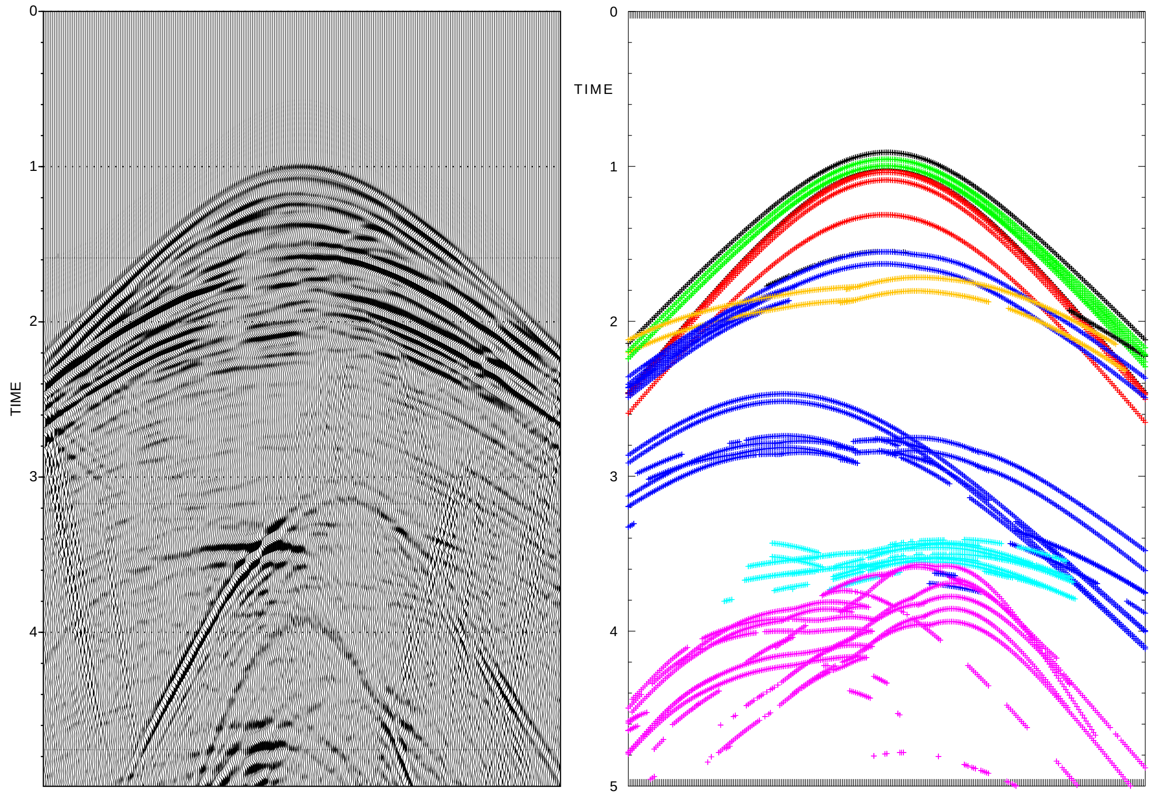

Finite-difference seismograms **Ray-theory travel times**

Figure 13. Ocean bottom cable, East-West direction, line 2.

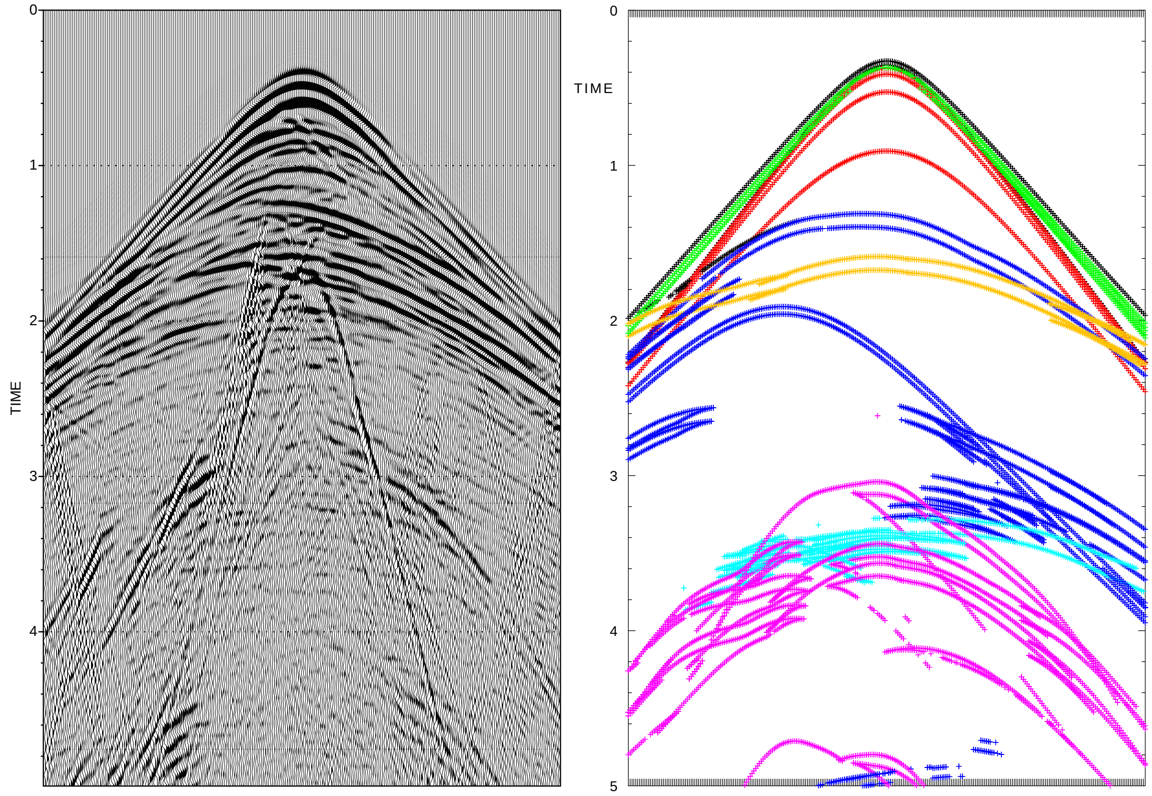

Finite-difference seismograms   Ray-theory travel times

Figure 14. Ocean bottom cable, East-West direction, line 3.

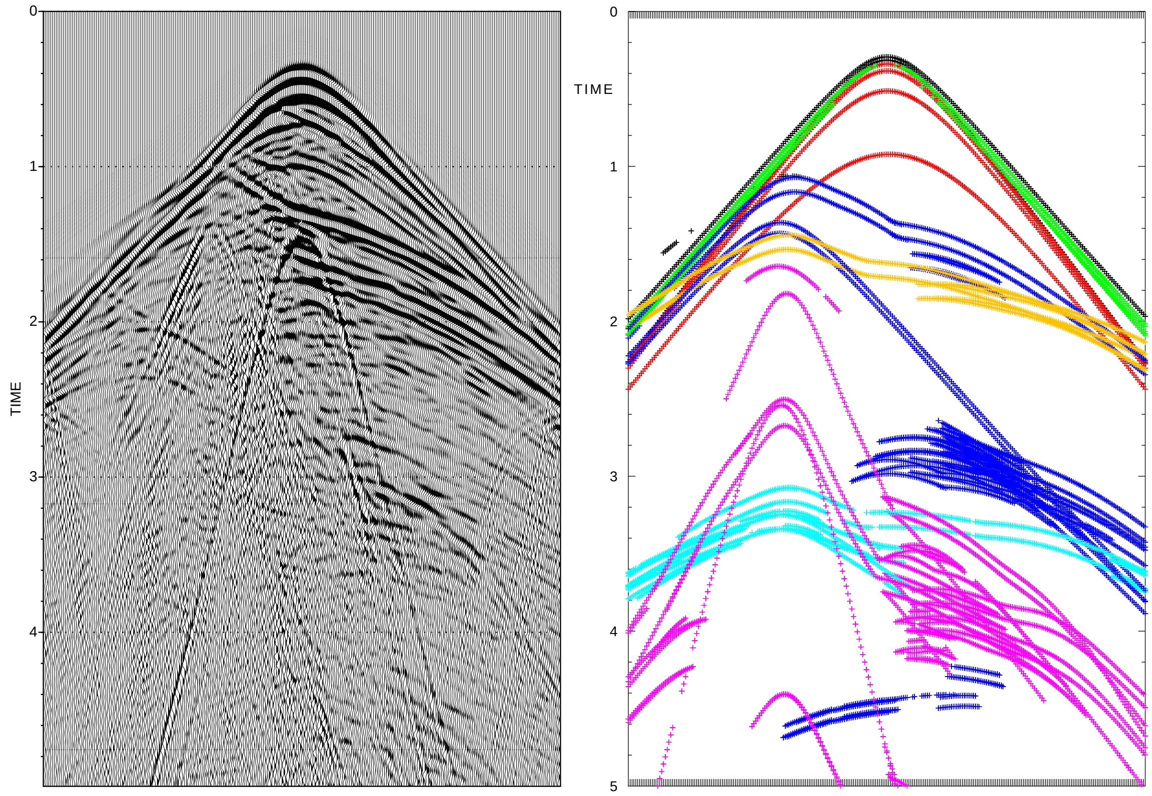

Finite-difference seismograms   Ray-theory travel times

Figure 15. Ocean bottom cable, East-West direction, line 4.

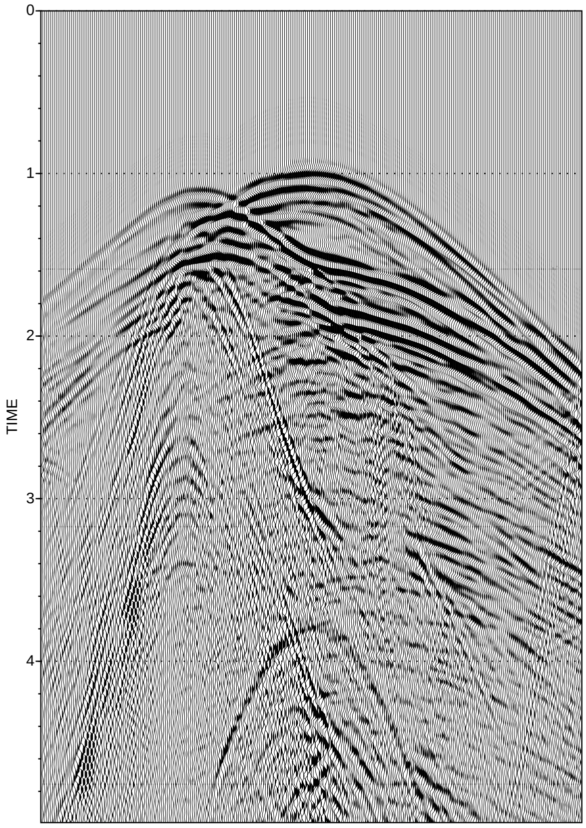

Finite-difference seismograms

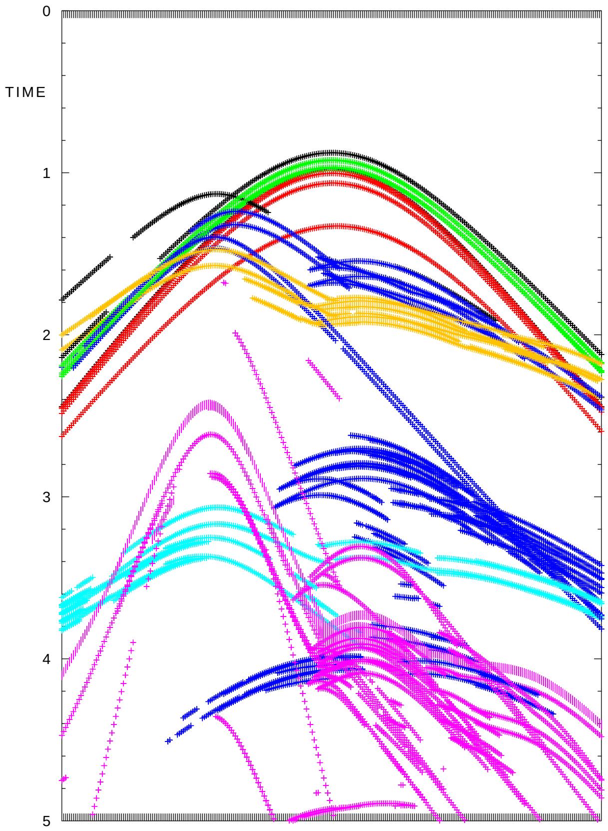

Ray-theory travel times

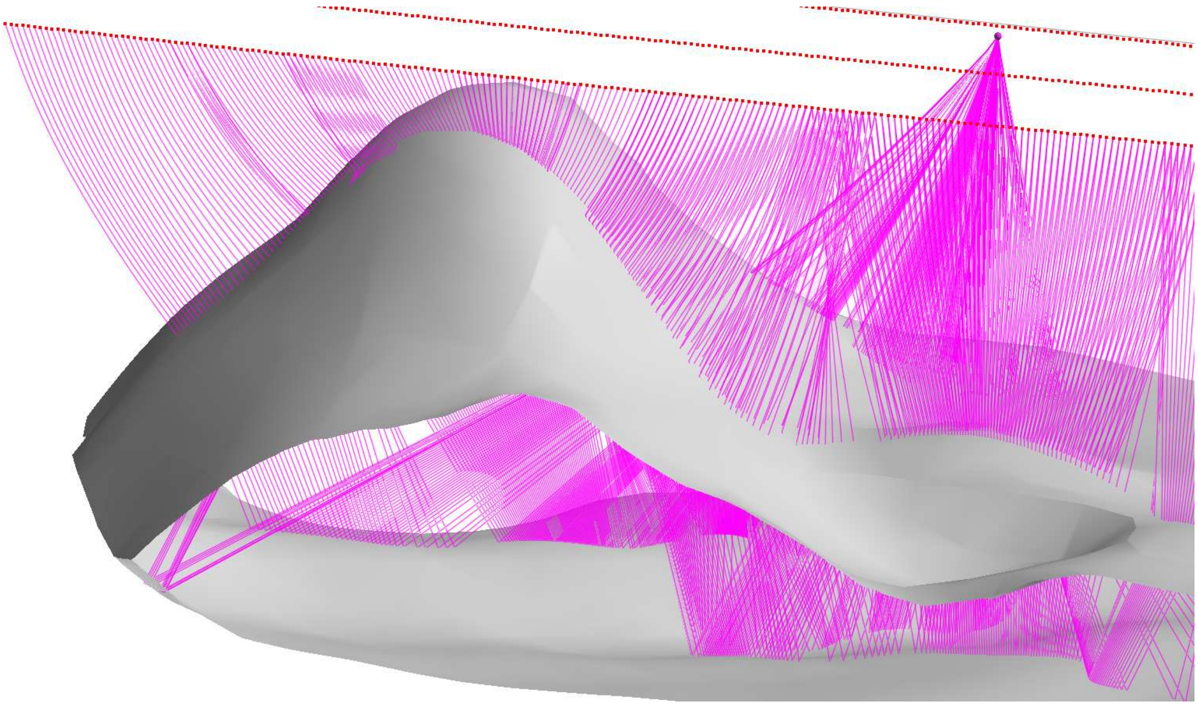

Rays of P-wave reflected and converted to S-wave at the bottom of the salt body.

Figure 16. Ocean bottom cable, East-West direction, line 5.

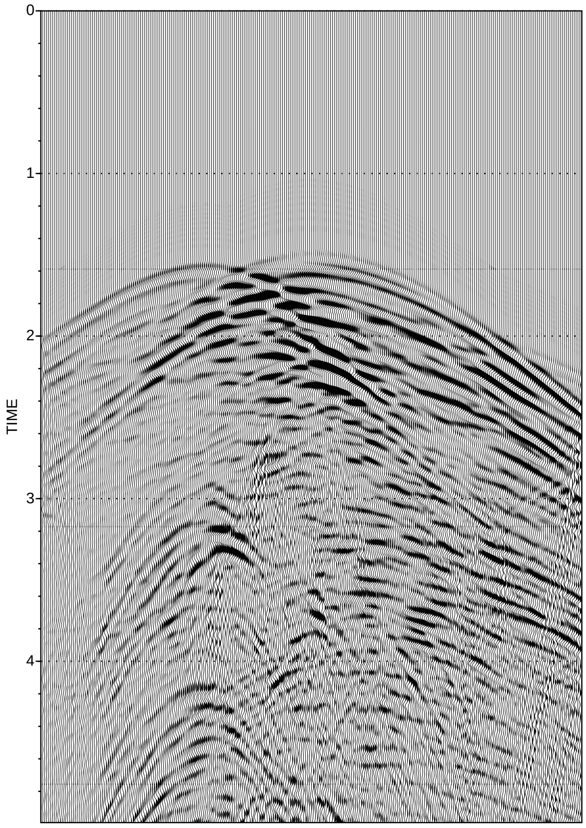

Finite-difference seismograms

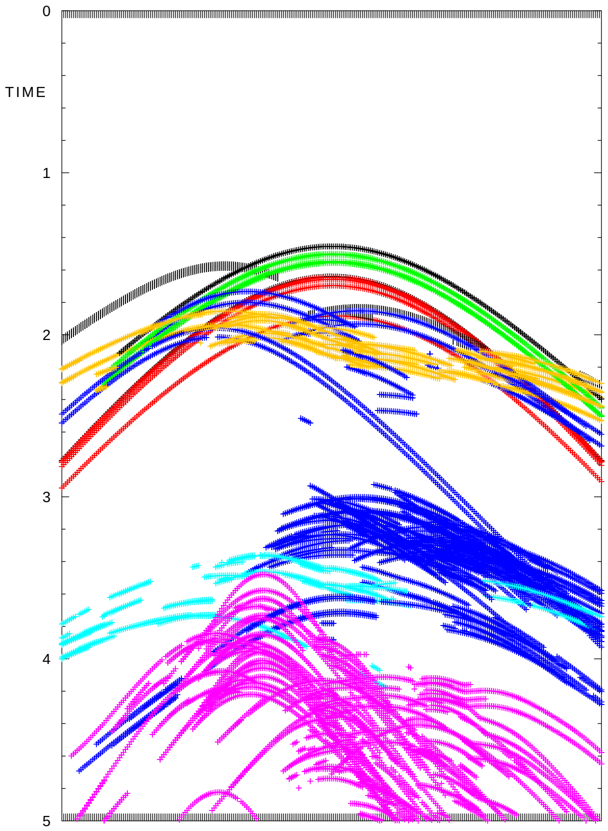

Ray-theory travel times

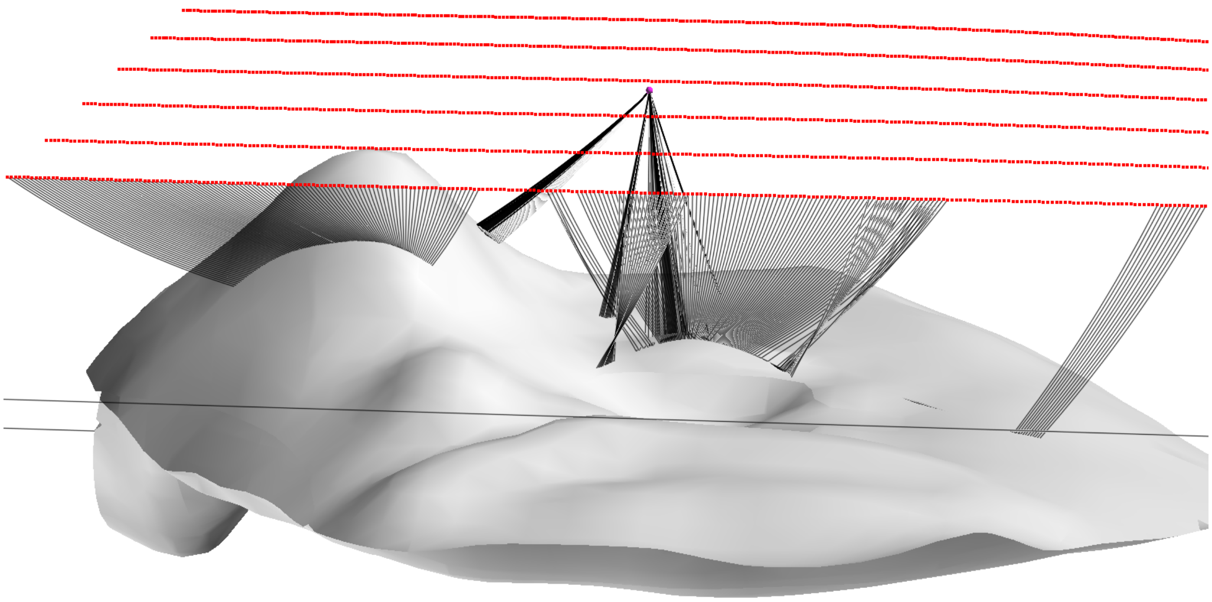

Rays of P-wave refracted in the salt body.

Figure 17. Ocean bottom cable, East-West direction, line 6.

5 Conclusions

Results of this paper demonstrate successful application of the SW3D software to two-point ray tracing and to calculation of ray-theory travel times in the smoothed elastic Salt Model with interfaces. The paper shows and explains some differences between finite-difference and ray-theory travel times for shot number 145 and five receiver configurations. Speed, low memory requirements, computation and visualization of ray paths and travel times of individual elementary waves are great advantages of the ray tracing method.

The time of the computation of travel times for one receiver line differs according to position in the model. The time for one marine streamer line was approximately nine hours and for one ocean bottom cable line approximately eleven hours on a PC equipped with an Athlon 64 3400+ (2.2 GHz) processor.

Acknowledgments

The author thanks Luděk Klimeš for valuable comments and recommendations concerning this paper.

The research was supported by the Grant Agency of the Czech Republic under Contract 205/04/1104, and by the members of the consortium "Seismic Waves in Complex 3-D Structures" (see "http://sw3d.mff.cuni.cz").

References

Bucha, V. (2005): Comparison of finite-difference and ray-theory seismograms in the elastic SEG/EAGE Salt Model, shot number 145. In: Seismic Waves in Complex 3-D Structures, Report 15, pp. 189–206, Dep. Geophys., Charles Univ., Prague.

Bulant, P. (2001): Sobolev scalar products in the construction of velocity models - application to model Hess, to SEG/EAGE Salt Model, and to model Pluto 1.5. In: Seismic Waves in Complex 3-D Structures, Report 11, pp. 133-159, Dep. Geophys., Charles Univ., Prague.

Bulant, P. (2002): Sobolev scalar products in the construction of velocity models: Application to model Hess and to SEG/EAGE Salt Model. Pure appl. Geophys., **159**, pp. 1487–1506.

Bulant, P. (2004): Constructing the SEG/EAGE 3-D Salt Model for ray tracing using Sobolev scalar products. Stud. Geophys. Geod., **48**, pp. 689–707.

Cohen, J.K. & Stockwell, Jr.J.W. (2004): CWP/SU: Seismic Un*x Release No. 38: a free package for seismic research and processing, Center for Wave Phenomena, Colorado School of Mines.

Červený, V., Klimeš, L. & Pšenčík, I. (1988): Complete seismic-ray tracing in three-dimensional structures. In: Doornbos, D.J.(ed.), Seismological Algorithms, Academic Press, New York, pp. 89–168.

House, S., Larsen, S. & Bednar, J.B. (2000): 3-D elastic numerical modeling of a complex salt structure. Exp. Abstr., Soc. Expl. Geophys. 70th Ann. Meet., pp. 2201-2204.

House, S., Larsen, S., Hoelting, C., Marfurt, K. & Wiley, R. (2004): Next-Generation Seismic Modeling and Imaging project: summary of elastic modeling results. Exp. Abstr., Soc. Expl. Geophys. 74th Ann. Meet., pp. 1869-1872.